HHS Public Access

Author manuscript

ACS Chem Biol. Author manuscript; available in PMC 2019 September 21.

Published in final edited form as:

ACS Chem Biol. 2018 September 21; 13(9): 2673–2681. doi:10.1021/acschembio.8b00610.

Rational Design of Potent Activators and Inhibitors of the *Enterococcus faecalis* Fsr Quorum Sensing Circuit

Dominic N. McBrayer, **Crissey D. Cameron**, **Brooke K. Gantman**, and **Yftah Tal-Gan***

Department of Chemistry, University of Nevada, Reno, 1664 N. Virginia Street, Reno, NV, 89557, USA.

Abstract

The increasing rate of resistance development to conventional antibiotics by bacteria necessitates the identification of alternative treatment possibilities that can reduce the ability of bacteria to adapt. *Enterococcus faecalis* remains the leading cause of clinical enterococci infections and has exhibited quorum sensing (QS)-dependent pathogenicity. Here we report the development of macrocyclic peptide-based activators and inhibitors of the *E. faecalis* Fsr QS circuitry. To this end, we developed, optimized, and compared three synthetic routes for lactone-containing macrocyclic peptide scaffolds. We then utilized previous and current structure-activity relationship (SAR) insights of the native QS signaling peptide to rationally design the most potent activators and inhibitors of the Fsr QS circuitry identified to date. The application of these peptides could provide a means to attenuate the pathogenicity of *E. faecalis* without introducing significant selective pressure on the bacteria to develop resistance.

Enterococcus faecalis, a commensal Gram positive bacterium, is an opportunistic pathogen that remains the leading cause of clinical enterococci infections, although *Enterococcus faecium* infections have been on the rise.[1–3] *E. faecalis* is normally found in the human intestinal tract, but can infect the blood (bacteremia), the urinary tract, and colonize the heart (endocarditis).[1, 2, 4–6] *E. faecalis* is inherently resistant to several antibiotics, and can rapidly develop or acquire new antibiotic resistances.[1, 6–8] In addition, *E. faecalis* has been shown to share resistance genes with other species, including multi-drug resistant strains such as methicillin-resistant *Staphylococcus aureus* (MRSA).[1] The costs associated with clinical *E. faecalis* infections along with the ability of *E. faecalis* to develop and share antibiotic resistance highlight the need to develop alternative strategies to eradicate *E. faecalis* infections.

One such alternative strategy to traditional antibiotics for combating bacterial infections is to develop molecules capable of attenuating the pathogenicity of the bacteria rather than

Corresponding Author ytalgan@unr.edu.

Notes

The authors declare no competing financial interest.

ASSOCIATED CONTENT

Supporting Information

Full details of experimental procedures, peptide characterization, and dose-response curves for all GBAP analogs. This material is available free of charge via the Internet at http://pubs.acs.org.

inducing cell death. This approach reduces the selective pressure to develop resistance while still eliminating many of the harmful effects of the bacteria.[9–13] *E. faecalis* is a tempting target for this approach as it has exhibited dependence on the use of quorum sensing (QS) to coordinate pathogenic group behaviors such as biofilm formation and virulence factor production.[14–17]

QS is a communication method used by bacteria to assess cell density and coordinate group behaviors including biofilm formation, virulence factor production, sporulation, competence induction, swarming, and bioluminescence.[10, 14, 18–22] QS in Gram positive bacteria relies on auto-inducing peptides (AIPs), which are produced and secreted by the bacteria. AIPs are used by bacteria to assess the local cell density and are responsible for activating the QS pathways. When the AIP concentration becomes sufficiently high, it activates a membrane-bound receptor, typically a histidine-kinase receptor, resulting in up-regulation of the QS genes (to synchronize the cells that are now engaging in group behaviors) as well as genes that activate group behaviors.[10, 14, 18–21, 23]

In *E. faecalis*, the master regulator of pathogenicity is termed the Fsr QS circuitry (Figure 1). This circuitry utilizes an 11-amino acid macrocyclic AIP termed gelatinase biosynthesis-activating pheromone (GBAP) to activate Fsr-dependent genes.[10, 14–16, 24] This peptide features a two-amino acid tail extending off the *N*-terminus of the peptide. The tail extends from a serine residue that is necessary for the formation of the lactone macrocyclic linkage between its side chain and the carboxylic acid of the *C*-terminal methionine residue. Structure-activity relationship (SAR) studies conducted by our group and others have identified key side chains and chiral orientations of those side chains, as well as sites that can tolerate modifications.[3, 25, 26] In addition, work has been done to assess the therapeutic potential of intercepting the Fsr QS circuitry as well as to develop a GBAP-based potent competitive inhibitor capable of attenuating *E. faecalis* QS-dependent pathogenecity.[27, 28]

In this study, we report the rational design of GBAP-based agonists and antagonists of the Fsr QS circuitry. To this end, we utilized previously reported SAR information to develop mechanistic hypotheses and implement them during the construction of abiotic GBAP analogs. This work has expanded the SAR knowledge of the GBAP molecule and resulted in the development of the most potent agonists and antagonists known to date with activities within the low to sub-nanomolar range.

RESULTS AND DISCUSSION

In our previous study, we identified several important structural elements that could be further refined as a first step towards the design of peptides with enhanced properties.[3] Thus, in this study we first evaluated the hydrophobic ring region as well as the exocyclic tail region of GBAP to gain additional SAR insights. We then utilized the combined SAR knowledge we gained to rationally design GBAP-based QS modulators with improved potencies.

Hydrophobic Ring Region (Steric) SAR Studies

To further refine the SAR insights regarding the ring region of GBAP (**1**), especially the role of Phe7, Gly8 and Trp10 in receptor binding and activation, we set out to evaluate these positions by including conservative point mutations. First, we found that replacement of Gly8 with alanine (GBAP-G8A, **2**) resulted in complete loss of activity.[3] As this modification effectively only added a chiral center, we hypothesized that the role of Gly8 is in allowing the peptide to assume a conformation that more resembles a D-amino acid in this position. Therefore, substitution of Gly8 with D-alanine should be more tolerated and result in an analog capable of effectively binding and activating the FsrC receptor. Indeed, replacement of Gly8 with D-alanine (GBAP-G8a, **3**) led to only a modest reduction in potency compared to the native GBAP (20-fold reduction in potency as opposed to complete loss of activity when L-alanine was placed in this position; Table 1).

Previously, we found that inverting the chirality at the Phe7 position (GBAP-f7, **4**) was surprisingly well tolerated (only 5-fold reduction in potency).[3] This result further supports our hypothesis that a D-amino acid-like orientation (accomplished by the flexibility afforded by glycine in native GBAP) is required in this region for GBAP to assume the bioactive conformation. Moreover, while this result could have been partially explained by the flexibility of the adjacent glycine, it is also possible that steric promiscuity in the receptor binding pocket allows effective binding of different side-chains and side-chain orientations at this position. To test this second possibility, analogs where Phe7 was substituted by tryptophan and D-tryptophan were prepared. It was found that tryptophan substitutions (F7W, **5** and F7w, **6**) were slightly more potent than their comparable phenylalanine analogs (Table 1). However, exchanging the native Trp10 and Phe7 residues to afford **7** (GBAP-F7WW10F) resulted in a 27-fold reduction in potency. Furthermore, substituting Trp10 with Phe (GBAP-W10F, **8**) resulted in an analog 5-fold less potent. Finally, replacement of both residues with alanine (GBAP-F7AW10A, **9**) resulted in complete loss of activity, a result that is in agreement with what has previously been reported.[26] Combined, these results emphasize the importance of the bulkier tryptophan side-chain at position 10, whereas the Phe7 residue is modifiable and could potentially be optimized to improve peptide-receptor binding. Moreover, the significant reduction in potency for **7** compared to the two, single replacement analogs (**5** and **8**) suggests that the residue exchange has resulted in a substantial conformational change compared with the native GBAP or the mono-substituted analogs. Lastly, the confirmed steric promiscuity of position 7 suggests that the Phe residue does not fully occupy its binding pocket in FsrC. However, the full extent of acceptable modifications in this position has not been determined.

Tail and Cyclization SAR Studies

We previously reported that an acetyl group (Figure 2A) is a sufficient exocyclic tail to maintain GBAP activity (**10**, Table 1).[3] Contrarily, a similar analog, lacking the tail, which was cyclized using a lactam ring (head-to-tail cyclization) was completely inactive (**11**),[3] while a D-amino acid mutation in Ser3 (GBAP-s3, **12**) resulted in 40-fold reduction in activity.[3] Combined, these results suggest that the chirality inversion of Ser3 led to a conformational change that resulted in the exocyclic tail clashing with the FsrC binding site. Thus, we hypothesized that replacing the tail with an acetyl group for this analog would lead

to improved activity. Indeed, Ac-GBAP-Des(Q1N2)s3 (**13**) exhibited a 6-fold increase in potency compared to the full-length analog (**12**). Interestingly, a lactam head-to-tail analog of **13** (compound **14**, Table 1) was also found to be more active than its L-Ser3 counterpart (**11**), suggesting that the inverted chirality in Ser3 induces a significant change in the ring conformation, even when the side chain is not directly involved in cyclization.

Previously, it was found that GBAP is prone to tail degradation to afford a pyroglutamate ring (Figure 2B) at the *N*-terminus.[3, 29, 30] We hypothesized that the inherent instability of GBAP could potentially have a regulatory role, allowing the bacteria to accurately detect changes in its population density. To test this hypothesis, we synthesized and evaluated both the D and L forms of the pyroglutamate degradation product. We found that the L-form (**15**) is comparable in activity to native GBAP, while the D-form (**16**) is about 3-fold less potent. These results refute the idea that the pyroglutamate degradation was selected for by evolutionary pressure and has a regulatory role in assessing population density.

Nakayama et al. reported the development of GBAP-based QS inhibitors, all of which contained a carboxy-benzyl (Z)-group (Figure 2C) protecting group at the *N*-terminus.[27] The authors claimed that the Z-group had no role in the activity of the analogs. To verify this, we set out to test the effect this group has on GBAP activity. In our experimental setup, we found that the addition of the Z-group to GBAP (Z-GBAP, **17**; Table 1) resulted in a 5-fold improvement in potency relative to native GBAP. Moreover, replacement of the exocyclic tail with the Z-group also led to a modest improvement in potency (Z-GBAP-Des(Q1N2) (**18**), 2-fold increase; Table 1). Combined, these results suggest that the addition of the Z-group should be considered when designing GBAP-based QS modulators with enhanced potencies.

Rational Design of GBAP-Based Super Agonists

In this study we aimed to develop GBAP analogs with enhanced potencies that could be utilized to modulate the Fsr QS circuitry. To this end, we first wanted to optimize the binding interactions between GBAP and the FsrC receptor. Our combined SAR studies of the GBAP signal revealed several side chain and chiral modifications that lead to approximately 5-fold improvement in peptide potency. These modifications include inversion of configuration at positions Gln1 and Asn2 (q1 and n2, respectively),[3] substitution of Pro4 with alanine (P4A),[3] and the addition of the Z-group at the *N*-terminus. We hypothesized that combining the modifications would have an additive effect and would thus lead to GBAP analogs with further enhancement in potency. We therefore synthesized a library of double and triple mutation analogs where we incorporated a combination of q1, n2, and P4A modifications, with or without an acetyl group at the *N*-terminus (Table 2). Our results indicate that the addition of an acetyl group, which had appeared to be a tolerated modification in our earlier study,[3] in combination with any of the above-mentioned modifications, results in decreased activity compared to the corresponding GBAP analogs without the acetyl group. Furthermore, several modifications were found to be incompatible with each other (for instance q1 and P4A), leading to analogs with reduced potency compared to GBAP. Most importantly, we identified two double mutation analogs (GBAP-

q1n2 (**19**) and GBAP-n2P4A (**21**)) that exhibit a significant improved activity (11- and 24-fold increase in potency compared to GBAP, respectively; Table 2).

In an attempt to further improve the two lead peptides identified above, we incorporated the Z-group to both scaffolds to afford Z-GBAP-q1n2 (**30**) and Z-GBAP-n2P4A (**31**) (Table 2). Interestingly, the incorporation of the Z-group in GBAP-q1n2 led to a modest 2-fold increase in potency, while the same mutation in GBAP-n2P4A led to a 3.5-fold decrease in potency (Table 2). These results are in agreement with the incompatibility of the q1 and P4A modifications described above and suggest that the P4A modification cannot tolerate either chiral inversion at the *N*-terminus residue, or *N*-terminus capping. Figure 3 summarizes the fold-change in potency (increase or decrease) of the rationally designed agonists compared to GBAP.

Development of GBAP-Based Antagonists

In addition to developing better agonists, we also sought to develop antagonists that could eventually lead to an alternative treatment for the attenuation of *E. faecalis* infections. Since a potent antagonist had been previously reported (**32**),[27] we used that structure as the starting scaffold for enhanced inhibitors development.

Surprisingly, the lead inhibitor that had been previously reported (**32**) was largely inactive in our hands, exhibiting an IC_{50} > 10,000 nM, even against a low competitor concentration (native GBAP, 5 nM). All the other tail-modified analogs in the same series were also inactive (Table 3; see below for a discussion on synthesis optimization as well as the steps taken to validate the surprisingly low activity observed for this series of compounds).

Since our synthetic method produces much higher yields and allows for faster synthesis by avoiding the in-solution cyclization steps, we developed a series of antagonist analogs with Gln9 reintroduced into the sequence as a resin attachment point. The single back-mutation analog (**36**) was well-tolerated and produced an antagonist with an IC_{50} of 227 nM in the presence of 50 nM GBAP as competitor. In an effort to better understand the SARs associated with the inhibitor that was previously reported,[27] we also conducted studies investigating the importance of the same tail modifications we made using the original scaffold (Table 3). We found that inclusion of a Z-group at the *N*-terminus had a slightly detrimental effect on inhibition activity as its removal (analog **35**) caused a slight increase in potency as seen by a roughly 1.5 to 2-fold decrease in the IC_{50} value relative to the analog containing the Z-group (**36**). Similarly, substituting a different capping group (acetyl, **38**) further reduced the potency relative to **35** by 3-fold. As mentioned previously, analogs with a free *N*-terminus can degrade to form the pyroglutamic acid residue.[3] As such, the degradation product was also tested (**37**) and resulted in an antagonist that was about 2-fold less potent relative to **35**. Likewise, removing the tail and capping the peptide (**39**) resulted in the least active analog in the series (about 6-fold loss in potency compared to **35**). Combined, these results provide an explanation as to why all the peptide analogs made based on the published scaffold (**32–34**)[27] were found to be inactive. The trend observed here suggests that only the free *N*-terminal analog, which we were unable to synthesize (see below), would be more active than the parent peptide scaffold (**32**).

During the enhanced agonist studies, we identified several modifications that significantly increase the binding affinity of GBAP to the FsrC receptor. We hypothesized that including the same modifications in our on-resin compatible inhibitors (**35** and **36**) would lead to enhancement of the inhibitors' potencies. Unfortunately, we found that this was not the case. All four antagonist analogs generated based on our two most potent agonists were less active than their parent compounds (**35** or **36**; Table 3). The antagonist analog that incorporated the q1n2 modification, along with the Z-group (**40**) was 2-fold less potent than **36**, while the antagonist analog that incorporated the n2 and P4A modifications, along with the Z-group (**41**) lost all inhibitory activity. Similarly, the analog that incorporated the q1n2 modification, without the Z-group (**42**) was about 7-fold less potent than **35**, while the analog that incorporated the n2P4A modifications, without the Z-group (**43**) also lost all inhibitory activity, similarly to **41**. Although the decreased potency of **41** was predictable based on the incompatibility of the P4A and Z-group modifications seen above (Table 2), the reduced potency of **40** compared to **36** as well as that of **42** and **43** compared to **35**, suggests that the tail modifications are not compatible with the ring modifications required to convert GBAP to a competitive inhibitor.

Minimal Modifications Needed to Produce an Antagonist

Following our discovery that reintroduction of Gln9 to the previously reported inhibitor (**32**) to afford **36** increased the potency by >50-fold, we set out to determine the minimal modifications required to convert GBAP to an inhibitor. Starting with **36**, the analog closest to the previously reported inhibitor (**32**) that is compatible with our entirely on-resin synthetic pathway, we first mutated back Met11 to afford **45**. This analog retained its inhibitory property but was >4-fold less potent than **36**. Since the removal of the Z-group from **36,** to afford **35**, resulted in a modest increase in potency while maintaining the inhibitory behavior, we hypothesized that removal of the Z-group from **45** would lead to an improved inhibitor. Indeed, **44** was found to be >2-fold more potent than **45** (Table 3). Interestingly, this analog, which differs from GBAP by only one residue (Asn5-to-benzyl-tyrosine (YBzl; Figure 2D)), was found to be a partial agonist, as it did not fully eliminate QS activity. Rather, **44** lowered QS activity by approximately 80%. This result emphasizes the importance of this modification to the conversion of GBAP to an inhibitor, but at the same time highlights the need for a second modification in order to fully eliminate agonistic activity. Moreover, the combined results of the antagonist library suggest that the tail region is more important for antagonistic activity than to agonistic activity, and that as a result, modifications of the tail region are less tolerated (compare activity trends of Tables 1 and 2 with that of Table 3).

Since we found that the benzyl-tyrosine modification is sufficient to convert GBAP into a partial inhibitor and that additional modifications are required to convert the peptide into a fully competitive inhibitor, we attempted to incorporate the enhanced agonist modifications (q1n2 or n2P4A) to this minimally-modified scaffold to afford **46** and **47**, respectively. Unfortunately, both analogs were found to be less potent than their parent scaffold (**44**) further emphasizing the incompatibility of the tail modifications with the benzyl-tyrosine ring modification.

Synthesis of Difficult-to-Make GBAP-Based Analogs

It was immediately apparent that our entirely on-resin synthetic method was incompatible with the scaffold on which **32** and its analogs were based as both resin attachment points (asparagine 5 and glutamine 9) used by our method had been removed by design (Scheme S-1). Thus, an alternative synthetic approach was needed. Initially, we followed the procedure referenced in the synthesis of the reported antagonist (Scheme S-1).[25, 27] However, in our hands, this approach gave extremely low yields and a high occurrence of epimerization at multiple sites on the peptide. In addition, as discussed above, compound **32** was found to be a much less active inhibitor than expected.

We hypothesized that the method of synthesis, particularly the difficult cyclization step, might be responsible for the inconsistencies observed in the activity. To help address both the yield issues and this inconsistency in observed potency, we developed an alternative synthetic approach that introduced some strategies from our entirely on-resin method by conducting the ester formation on-resin and then conducting a facile cyclization in-solution through amide formation (Scheme S-1). The peptide (**32**) prepared using this alternative method remained inactive, suggesting that differences in the synthetic approach are not the cause of the much lower activity that was reproducibly observed in our hands. In addition, when the most similar peptide that was compatible with our entirely on-resin synthesis (**36)** was resynthesized using the same method used to produce **32**, **36** retained its potency. Combined, these results reinforce the validity of our synthetic approach and the observed lack of activity of **32** in our hands.

Although the synthetic modifications we introduced allowed us to prepare most of the planned peptides, including **32**, we were still unable to prepare one planned analog, lacking an *N*-terminal capping group, due to extremely low yields associated with the extra steps involved with deprotecting the *N*-terminus following in-solution cyclization (see SI for description of methods employed for this specific peptide). Also, while the modified synthetic method reduced the production of isomers to a more reasonable level, at least one significant and difficult-to-remove contaminant (an isomer), remained (this isomer was tested and found to be inactive).

Evaluating a Lead Antagonist in a Phenotypic Assay

While our reporter assays have established the ability of our peptides to modulate the QS response, we wanted to also verify that this could translate into modulation of a therapeutically important phenotype. To address this, we tested the ability of the lead antagonist, **35**, to attenuate biofilm formation in wild type *E. faecalis* cells (strain TX4002). Since biofilm formation can also be influenced by other pathways, we included a QS-inactive strain (TX5266) for comparison (Figures 4 and S-1). We found that adding exogenous GBAP to cells increased the amount of biofilm formation by about 30–50%. However, regardless of whether exogenous GBAP was included or not, inclusion of **35** at concentrations 5-fold greater than its IC_{50} was sufficient to reduce biofilm formation to the levels of the QS-inactive strain (a reduction of about 30–50%). These results demonstrate the ability of the antagonist to completely abolish the QS-dependent formation of biofilm, even when there is sufficient native activator present to fully induce a QS response.

Conclusions

We utilized current and previous SAR knowledge of the GBAP signal to rationally design GBAP-based QS modulators with enhanced activities. To this end, we developed, optimized, and compared three synthetic routes for the construction of GBAP analogs. Our results indicate that the entirely on-resin synthetic method is superior to the two solution-based cyclization methods in efficiency, ease of purification, and overall yield.

Our designed enhanced agonist library yielded several analogs with significantly improved activities (>20-fold increase in potency). This library also revealed several modifications that are not compatible with each other and thus result in a decrease in potency when combined. It is tempting to speculate that the reason for the incompatibility is due to steric clashing introduced by the conformational changes that each modification induced, however additional structural studies are required to confirm that. Figure 5 summarizes the key SAR conclusions obtained from the agonist library.

With regard to GBAP-based competitive inhibitors, we have found that a single modification (N5[YBzl]) is sufficient to convert GBAP to a potent inhibitor with an IC_{50} value in the nanomolar range, even in the presence of a significant concentration of native competitor. This result emphasizes the need to validate all modifications in order to correctly attribute the SARs that are observed to their associated modification (the earlier study that used a reverse-alanine scan approach was able to identify this unexpected modification as being important, but put greater emphasis on alanine substitutions as contributors to the SARs they observed).[27] Our systematic analysis of GBAP-based antagonists revealed potent inhibitors with improved potencies of >50-fold compared to the previously reported lead compound (**32**). These new analogs are thus privileged scaffolds for the design of GBAP-based QS inhibitors with potential therapeutic implications. Indeed, our lead inhibitor, **35**, was able to fully inhibit a pathogenic phenotype, biofilm formation, in a wild-type *E. faecalis* strain to levels comparable to a QS-inactive strain.

Combined, the SAR insights gained in this study suggest several areas for either additional improvement in binding or possible modifications that are well tolerated and might be useful for improving the stability of the peptide analogs. First, incorporating additional D-amino acids at tolerated sites (such as Phe7) could improve stability of the peptide against protease degradation. The advantages in stability may offset the associated mild loss in potency, especially in peptides that are already highly potent. Incorporating a D-Trp substitution for Phe7, which was nearly as potent as the native peptide could potentially grant increased peptide stability at minimal cost to potency. Second, the exocyclic tail region has the capacity to significantly alter potency in both agonists and antagonists. This could be achieved either by altering the stereochemistry of the exocyclic tail residues or through *N*-terminus capping. Such experiments, aimed at further improving agonist and antagonist potencies, along with in-depth structural studies aimed at determining the molecular mechanism that drive GBAP-FsrC binding and result in FsrC activation, are on-going in our laboratory and will be reported in due course.

METHODS

General.

All peptides were purified to ≥ 95% as confirmed by analytical reverse phase high-performance liquid chromatography (RP-HPLC). See Tables S-1 and S-2 for individual purities of all peptides.

Peptide Synthesis.

Entirely on-resin Fluorenylmethyloxycarbonyl (Fmoc)-based peptide synthesis[31–33] was conducted as we previously described (see SI for full details). For analogs that were incompatible with this method of synthesis, two approaches that mixed on-resin linear synthesis and in-solution cyclization reactions were utilized to prepare the peptides. In-solution cyclization attempts were initially followed, as previously published, using a two-fold excess mass of 4-dimethylaminopyridine (DMAP) and benzotriazol-1-yl-oxytripyrrolidinophosphonium hexafluorophosphate (PyBOP) to crude peptide (e.g. 2 mg of base and coupling reagent for every 1 mg of crude peptide),[25] without success, due to rampant epimer formation.

The following method reduced the formation of epimer side products: The linear peptide sequence was prepared on Ala-loaded Wang resin (Chem-Impex) using common *N*,*N*,*N*′,*N*′-tetramethyl-O-(1H-benzotriazol-1-yl)uranium hexafluorophosphate (HBTU)-based methods. The peptide was then cleaved and precipitated, and the crude mass was recorded for calculations of equivalents assuming 100% yield of the desired product. The crude peptide was dissolved in *N*,*N*-dimethylformamide (DMF) to form a 0.5 to 1 mg mL^{-1} solution (low concentrations were used in an effort to minimize inter-peptide polymerization). 1.25 equiv of PyBOP and 2.5 equiv of *N*,*N*-Diisopropylethylamine (DIPEA) were added to this peptide solution. The solution was stirred vigorously for 16 – 24 hours. At this point, another 1.25 equiv of PyBOP, 2.5 equiv of DIPEA, and 0.01 equiv of DMAP were added, and the solution stirred an additional 4 to 6 hours before undergoing purification.

Despite the reduction in epimer formation seen in the above off-resin cyclization conditions, efforts were made to further reduce the unwanted side products. To this end, for peptides that were not compatible with the entirely on-resin method and that were capped at the *N*-terminus, we developed an alternative path to cyclization through amide formation rather than through the ester. The ester was instead formed on-resin using methods we have reported previously.[3] These peptides were synthesized starting either with Ala or Phe-loaded Wang resin (Chem-Impex). As with the entirely on-resin method, Ser(Trt) was incorporated at position three while Z-Gln was added at the tail. Ester formation was accomplished as previously reported,[3] and the remainder of the linear peptide sequence was then extended using standard coupling methods for these peptides (see SI). After cleavage from the resin, the crude mass was weighed and equivalents of reagents were calculated assuming 100% of the desired peptide. An approximately 0.5 to 1 mg/mL solution of crude peptide in DMF was treated with 1.25 equiv of PyBOP and 2.5 equiv of DIPEA and stirred vigorously for 4 hours. The peptide was then purified.

Peptide Purification and Verification.

Peptides that could not be synthesized using the entirely on-resin method needed to be removed from the DMF used for the in-solution cyclization reactions prior to purification. To remove the DMF used as a reaction solvent, as well as polar contaminants, off-resin cyclization reactions were diluted with water to produce a ≤ 25% (v/v) DMF solution (usually a 4- to 5-fold dilution). This solution was then flowed through a 100 mg-capacity C18 cartridge (Waters) in portions that would concentrate approximately 5–10 mg of peptide. The cartridge was then washed with 5 – 10 mL 20% (v/v) acetonitrile (ACN) in water. The peptide was then eluted by passing through 3 – 6 mL of 95% (v/v) ACN in water and collected. The cartridge was washed with 5 – 10 mL of 5% (v/v) ACN in water. The steps in this process were repeated until all the original diluted solution had been loaded, washed, and eluted. The eluted fractions were combined and lyophilized prior to being purified further using RP-HPLC. Peptide purification by RP-HPLC and verification by mass spectrometry (MS) were conducted as previously described (see SI).[3]

β-Galactosidase Reporter Assay.

To quantify the activation of the QS circuit, as seen by activation of the *gelE* promoter, a β-galactosidase reporter assay was used. This assay was conducted as previously described for the determination of EC_{50} values.[3] Briefly, *E. faecalis* TX5274 bacteria were grown on Mueller-Hinton Broth 2 (MHB-2) plates without antibiotics overnight at 37 °C. An isolated colony was then transferred to 5 mL of brain heart infusion (BHI) broth containing 500 μg/mL of kanamycin and shaken overnight at 37 °C in ambient atmosphere. These overnight cultures were then diluted 50-fold into BHI broth with a final concentration of 500 μg/mL kanamycin. The cells were then grown with shaking at 37 °C for 1 h before 198 μL aliquots were placed in the wells of a 96-well plate containing either 2 μL dimethyl sulfoxide (DMSO) or 2 μL experimental peptide dissolved in DMSO and statically incubated at 37 °C for 2 h. The experimental peptide concentrations were varied along a 9-point, 5-fold serial dilution starting with 10 μM and ending with 0.052 nM. In cases where the initial sigmoidal curve gave few baseline points, the starting point for the 9-point dilution series was adjusted and the dilution varied between 2-fold, 3-fold, or 5-fold as necessary. Each well was treated with 2 μL DMSO solution of experimental peptide, GBAP positive control, or DMSO negative control. After the incubation time had elapsed, the absorbance at 600 nm (A600) was read. The wells were then treated with 20 μL of 1% (v/v) Triton X-100 in water for 30 min at 37 °C to lyse the cells. After lysis, 100 μL of the lysate was transferred to a new well containing 100 μL substrate buffer containing 0.8 mg/mL ortho-Nitrophenyl-β-galactoside (ONPG) and 2.7 μL mL^{-1} β-mercaptoethanol in Z-buffer (100 mM sodium phosphate buffer, 10 mM KCl, and 1 mM MgSO4, pH 7.0). The enzyme reaction was run for 30 min at 37 °C before being quenched with 20 μL of 1 M sodium carbonate in water. The absorbance of quenched reaction wells was read at 420 nm (A420) and 550 nm (A550), allowing for the calculation of the activity in Miller units (Equation 1).

$$Miller\ Unit = 1000 * \frac{A420 - c * A550}{t * v * A600} \quad \text{Equation 1:}$$

Where c is a species-specific correction factor (1.6 for *E. faecalis*), t is the substrate reaction time in minutes, and v is the volume of lysed cell culture used in the enzyme reaction in milliliters.[16] The equation allows for correction of background absorbance due to initial cell density, cell lysate turbidity, and enzyme reaction time.

After Miller unit determination, the average value for the DMSO negative control was subtracted and the results normalized to the average value of the GBAP positive control. The EC_{50} value was determined through fitting using nonlinear regression with GraphPad Prism using Equation 2.

$$y = min + \frac{\max - min}{1 + 10^{\log(EC50 - x)}} \quad \text{Equation 2}$$

Where min is the average minimum signal and max is the average maximum signal. If the maximum concentration (10 μM) activity of a peptide was less than or equal to 50% relative to the GBAP positive control, that peptide was tested as a potential competitive inhibitor. The IC_{50} of antagonistic peptides was determined similarly. However, each sample also included 5 or 50 nM of GBAP as a competitor standard. The 50 nM concentration of GBAP was determined to reproducibly give 90 – 95% of the GBAP maximum signal while the 5 nM concentration was used to evaluate the effectiveness of select antagonists if they were to be applied before QS was fully established. After Miller unit determination, the DMSO negative control was subtracted and the results were normalized to the signal produced by the concentration of competing GBAP used in the absence of any potential inhibitor. All experiments were conducted in triplicate and repeated on three separate days.

Acknowledgements

This work was supported by the Nevada INBRE through a grant from the National Institutes of Health (GM103440), the National Science Foundation (CHE-1808370), the National Institutes of Health (R35GM128651), and by the Cayman Biomedical Research Institute (CaBRI). The *E. faecalis* reporter strain, TX5274, wild type strain, TX4002, and the QS-inactive strain, TX5266, were kindly provided by B. Murray (University of Texas Health Science Center, Houston).

Abbreviations Used

ACN	acetonitrile
AIP	auto-inducing peptide
BHI	brain heart infusion
DIPEA	*N,N*-Diisopropylethylamine
DMAP	4-dimethylamiopyridine
DMF	*N,N*-dimethylformamide
DMSO	dimethyl sulfoxide
Fmoc	Fluorenylmethyloxycarbonyl

GBAP	gelatinase biosynthesis-activating pheromone
HBTU	*N*,*N*,*N*′,*N*′-tetramethyl-O-(1H-benzotriazol-1-yl)uranium hexafluorophosphate
MRSA	methicillin-resistant *Staphylococcus aureus*
MS	mass spectrometry
ONPG	ortho-Nitrophenyl-β-galactoside
PyBOP:	benzotriazol-1-yl-oxytripyrrolidinophosphonium hexafluorophosphate
QS	quorum sensing
RP-HPLC	reverse phase high performance liquid chromatography
SAR	structure-activity relationship
YBzl	Benzyl-tyrosine
Z	carboxy-benzyl

References

[1]. Huycke M, Sahm D, and Gilmore MS (1998) Multiple-Drug Resistant Enterococci: The Nature of the Problem and an Agenda for the Future, Emerging Infect. Dis 4, 239–249. [PubMed: 9621194]

[2]. Arias CA, and Murray BE (2012) The rise of the Enterococcus: beyond vancomycin resistance, Nat. Rev. Microbiol 10, 266–278. [PubMed: 22421879]

[3]. McBrayer DN, Gantman BK, Cameron CD, and Tal-Gan Y (2017) An Entirely Solid Phase Peptide Synthesis-Based Strategy for Synthesis of Gelatinase Biosynthesis-Activating Pheromone (GBAP) Analogue Libraries: Investigating the Structure–Activity Relationships of the Enterococcus faecalis Quorum Sensing Signal, Org. Lett 19, 3295–3298. [PubMed: 28590764]

[4]. Fisher K, and Phillips C (2009) The ecology, epidemiology and virulence of Enterococcus, Microbiol. SGM 155, 1749–1757.

[5]. Van Tyne D, and Gilmore MS (2014) Friend Turned Foe: Evolution of Enterococcal Virulence and Antibiotic Resistance, Annu. Rev. of Microbiol 68, 337–356. [PubMed: 25002090]

[6]. O'Driscoll T, and Crank CW (2015) Vancomycin-resistant enterococcal infections: epidemiology, clinical manifestations, and optimal management, Infect. Drug Resist 8, 217–230. [PubMed: 26244026]

[7]. Paulsen IT, Banerjei L, Myers GSA, Nelson KE, Seshadri R, Read TD, Fouts DE, Eisen JA, Gill SR, Heidelberg JF, Tettelin H, Dodson RJ, Umayam L, Brinkac L, Beanan M, Daugherty S, DeBoy RT, Durkin S, Kolonay J, Madupu R, Nelson W, Vamathevan J, Tran B, Upton J, Hansen T, Shetty J, Khouri H, Utterback T, Radune D, Ketchum KA, Dougherty BA, and Fraser CM (2003) Role of mobile DNA in the evolution of vancomycin-resistant Enterococcus faecalis, Science 299, 2071–2074. [PubMed: 12663927]

[8]. Lim S-K, Tanimoto K, Tomita H, and Ike Y (2006) Pheromone-responsive conjugative vancomycin resistance plasmids in Enterococcus faecalis isolates from humans and chicken feces, Appl. Environ. Microbiol 72, 6544–6553. [PubMed: 17021204]

[9]. Gerdt JP, and Blackwell HE (2014) Competition Studies Confirm Two Major Barriers That Can Preclude the Spread of Resistance to Quorum-Sensing Inhibitors in Bacteria, ACS Chem. Biol 9, 2291–2299. [PubMed: 25105594]

[10]. Rutherford ST, and Bassler BL (2012) Bacterial Quorum Sensing: Its Role in Virulence and Possibilities for Its Control, Cold Spring Harbor Perspect. Med 2, a012427.

[11]. Tang K, and Zhang X-H (2014) Quorum Quenching Agents: Resources for Antivirulence Therapy, Mar. Drugs 12, 3245–3282. [PubMed: 24886865]

[12]. Garland M, Loscher S, and Bogyo M (2017) Chemical Strategies To Target Bacterial Virulence, Chem. Rev (Washington, DC, U. S.) 117, 4422–4461. [PubMed: 28234447]

[13]. Johnson BK, and Abramovitch RB (2017) Small Molecules That Sabotage Bacterial Virulence, Trends Pharmacol. Sci 38, 339–362. [PubMed: 28209403]

[14]. Cook LC, and Federle MJ (2014) Peptide pheromone signaling in Streptococcus and Enterococcus, FEMS Microbiol. Rev 38, 473–492. [PubMed: 24118108]

[15]. Qin X, Singh KV, Weinstock GM, and Murray BE (2000) Effects of Enterococcus faecalis fsr genes on production of gelatinase and a serine protease and virulence, Infect. Immun 68, 2579–2586. [PubMed: 10768947]

[16]. Qin X, Singh KV, Weinstock GM, and Murray BE (2001) Characterization of fsr, a regulator controlling expression of gelatinase and serine protease in Enterococcus faecalis OG1RF, J. Bacteriol 183, 3372–3382. [PubMed: 11344145]

[17]. Pinkston KL, Gao P, Diaz-Garcia D, Sillanpaeae J, Nallapareddy SR, Murray BE, and Harvey BR (2011) The Fsr Quorum-Sensing System of Enterococcus faecalis Modulates Surface Display of the Collagen-Binding MSCRAMM Ace through Regulation of gelE, J. Bacteriol 193, 4317–4325. [PubMed: 21705589]

[18]. Papenfort K, and Bassler BL (2016) Quorum sensing signal-response systems in Gram-negative bacteria, Nat. Rev. Microbiol 14, 576–588. [PubMed: 27510864]

[19]. Turan NB, Chormey DS, Büyükpınar Ç, Engin GO, and Bakirdere S (2017) Quorum sensing: Little talks for an effective bacterial coordination, TrAC, Trends Anal. Chem 91, 1–11.

[20]. Yang Y, Koirala B, Sanchez LA, Phillips NR, Hamry SR, and Tal-Gan Y (2017) Structure–Activity Relationships of the Competence Stimulating Peptides (CSPs) in Streptococcus pneumoniae Reveal Motifs Critical for Intra-group and Cross-group ComD Receptor Activation, ACS Chem. Biol 12, 1141–1151. [PubMed: 28221753]

[21]. Harrington A, and Tal-Gan Y (2018) Identification of Streptococcus gallolyticus subsp. gallolyticus (biotype I) competence stimulating peptide pheromone, J. Bacteriol., JB 00709–00717.

[22]. Abisado RG, Benomar S, Klaus JR, Dandekar AA, and Chandler JR (2018) Bacterial Quorum Sensing and Microbial Community Interactions, mBio 9, e02331–02317. [PubMed: 29789364]

[23]. Mull RW, Harrington A, Sanchez LA, and Tal-Gan Y (2018) Cyclic Peptides that Govern Signal Transduction Pathways: From Prokaryotes to Multi-Cellular Organisms, Curr. Top. Med. Chem (Sharjah, United Arab Emirates)

[24]. Nakayama J, Cao Y, Horii T, Sakuda S, Akkermans ADL, de Vos WM, and Nagasawa H (2001) Gelatinase biosynthesis-activating pheromone: a peptide lactone that mediates a quorum sensing in Enterococcus faecalis, Mol. Microbiol 41, 145–154. [PubMed: 11454207]

[25]. Nakayama J, Cao Y, Horii T, Sakuda S, and Nagasawa H (2001) Chemical synthesis and biological activity of the gelatinase biosynthesis-activating pheromone of Enterococcus faecalis and its analogs, Biosci., Biotechnol., Biochem 65, 2322–2325. [PubMed: 11758932]

[26]. Nishiguchi K, Nagata K, Tanokura M, Sonomoto K, and Nakayama J (2009) Structure-Activity Relationship of Gelatinase Biosynthesis-Activating Pheromone of Enterococcus faecalis, J. Bacteriol 191, 641–650. [PubMed: 18996993]

[27]. Nakayama J, Yokohata R, Sato M, Suzuki T, Matsufuji T, Nishiguchi K, Kawai T, Yamanaka Y, Nagata K, Tanokura M, and Sonomoto K (2013) Development of a Peptide Antagonist against fsr Quorum Sensing of Enterococcus faecalis, ACS Chem. Biol 8, 804–811. [PubMed: 23362999]

[28]. Garsin DA, Sifri CD, Mylonakis E, Qin X, Singh KV, Murray BE, Calderwood SB, and Ausubel FM (2001) A simple model host for identifying Gram-positive virulence factors, Proc. Natl. Acad. Sci. U. S. A 98, 10892–10897. [PubMed: 11535834]

[29]. Chelius D, Jing K, Lueras A, Rehder DS, Dillon TM, Vizel A, Rajan RS, Li T, Treuheit MJ, and Bondarenko PV (2006) Formation of Pyroglutamic Acid from N-Terminal Glutamic Acid in Immunoglobulin Gamma Antibodies, Anal. Chem 78, 2370–2376. [PubMed: 16579622]

[30]. Povoledo D, and Vallentyne JR (1964) Thermal reaction kinetics of the glutamic acid-pyroglutamic acid system in water, Geochim. Cosmochim. Acta 28, 731–734.

[31]. (2000) Fmoc solid phase peptide synthesis: a practical approach, Oxford University Press, New York.

[32]. Behrendt R, White P, and Offer J (2016) Advances in Fmoc solid-phase peptide synthesis, J. Pept. Sci 22, 4–27. [PubMed: 26785684]

[33]. Chantell CA, Onaiyekan MA, and Menakuru M (2012) Fast conventional Fmoc solid-phase peptide synthesis: a comparative study of different activators, J. Pept. Sci 18, 88–91. [PubMed: 22147296]

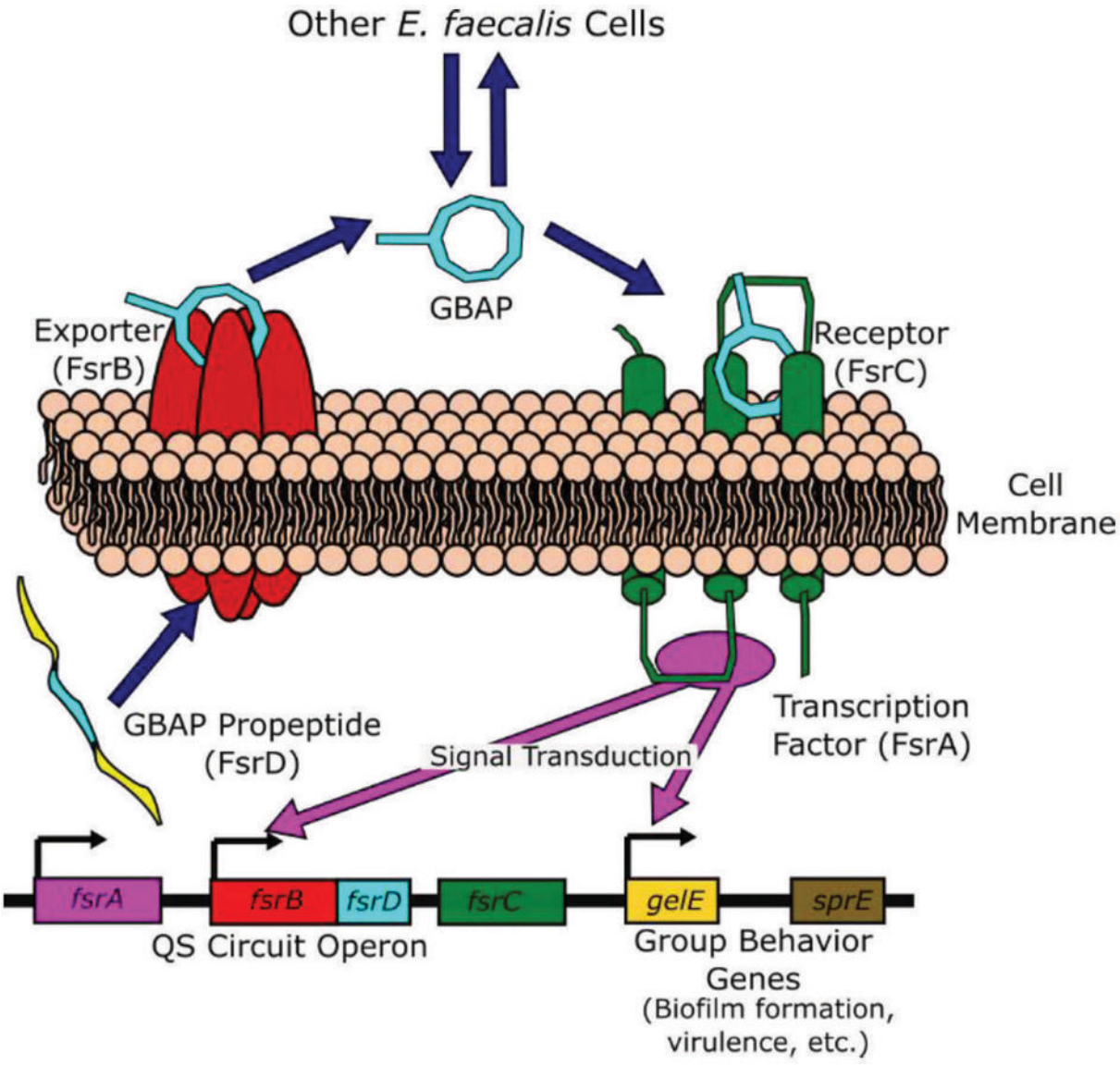

Figure 1.

The *E. faecalis* Fsr QS circuit: When GBAP binds to the membrane-bound histidine-kinase receptor FsrC, the transcription factor FsrA is phosphorylated, resulting in upregulation of the exporter, FsrB, the GBAP propeptide FsrD, and FsrC (autoinduction). In addition, the group behavior genes *gelE* and *sprE* are upregulated, resulting in the production of virulence factors such as gelatinase and the formation of biofilms. The linear GBAP propeptide is processed into the mature macrocycle and exported by FsrB.

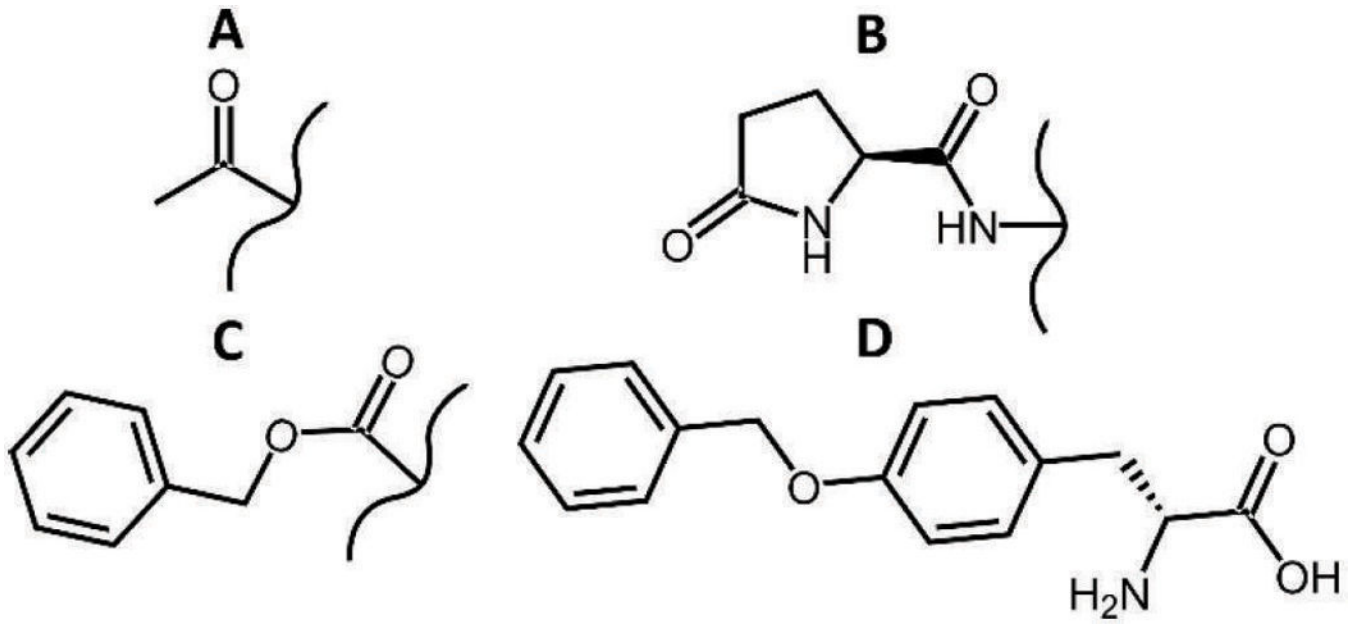

Figure 2.

Less common functional groups incorporated in this study include the A) acetyl *N*-terminal capping group, B) pyroglutamate *N*-terminal degradation product, C) carboxy-benzyl (Z) *N*-terminal capping group, D) benzyl-tyrosine (YBzl) non-proteinogenic amino acid.

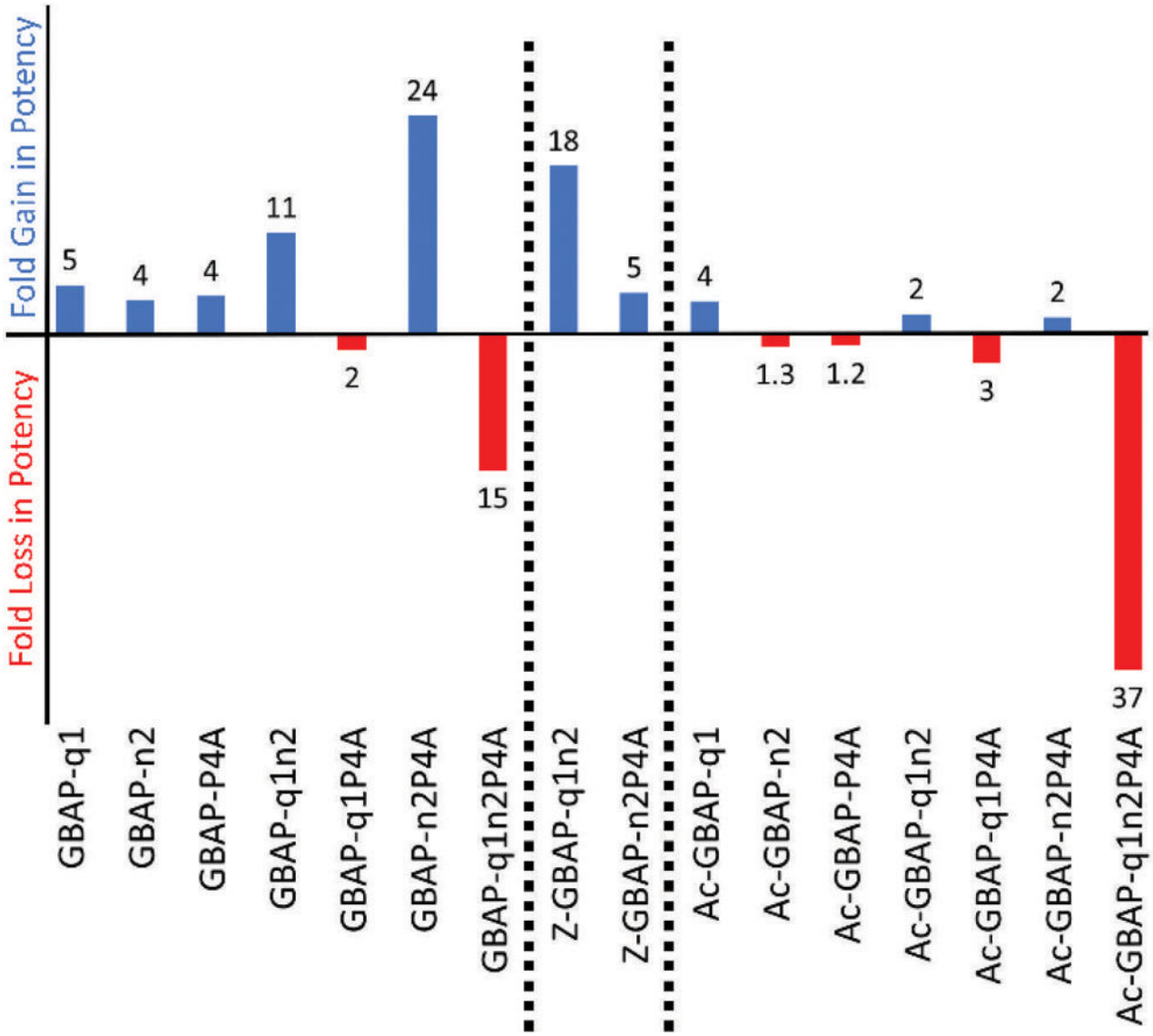

Figure 3.

Fold enhancement (blue) or reduction (red) in potency for analogs compared to GBAP to demonstrate effect of modifications on altering the agonist potency compared to the native peptide.

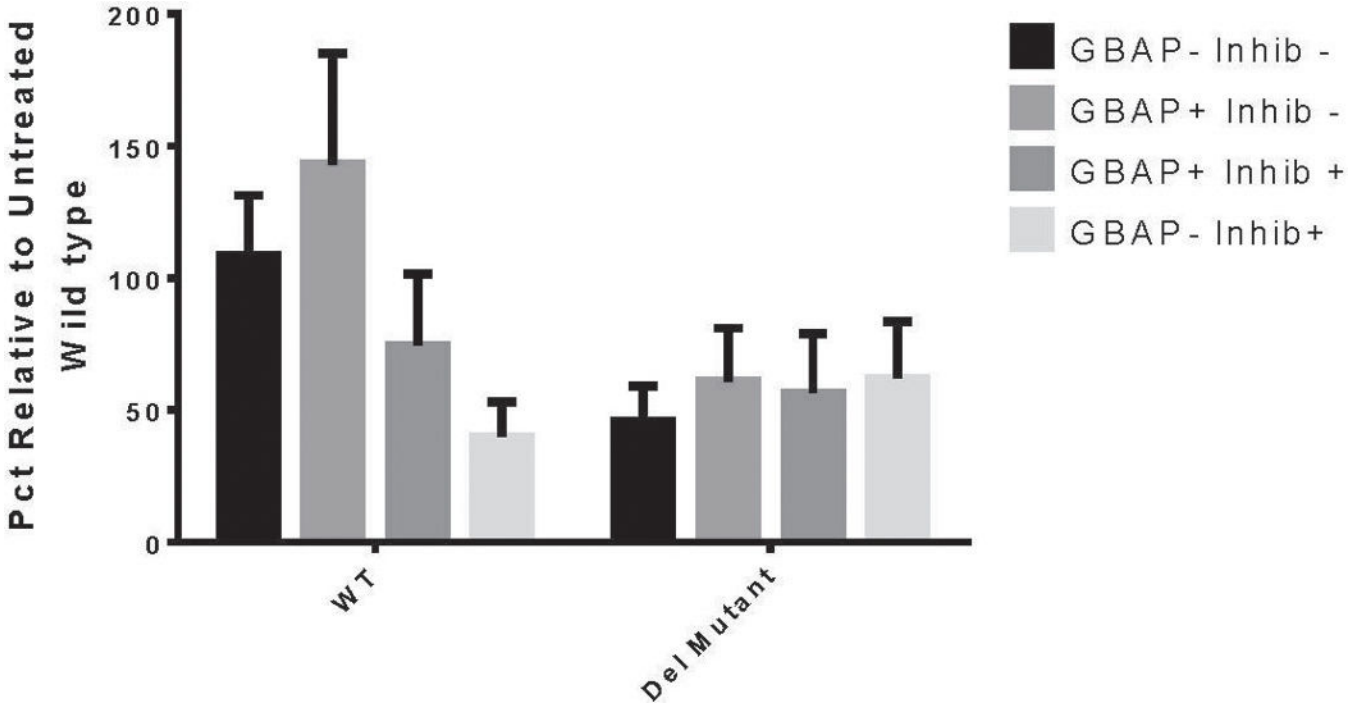

Figure 4.

Inhibition of biofilm formation by antagonistic GBAP analog. Wild type *E. faecalis* (TX4002) results are compared with a QS-inactive deletion mutant (TX5266). Addition of exogenous GBAP without inhibitor (GBAP+ Inhib-) increases biofilm formation above wild type levels. Treatment with the inhibitor GBAP-N5[YBzl]M11A (**35**) reduces biofilm production to QS-inactive levels for all wild type samples.

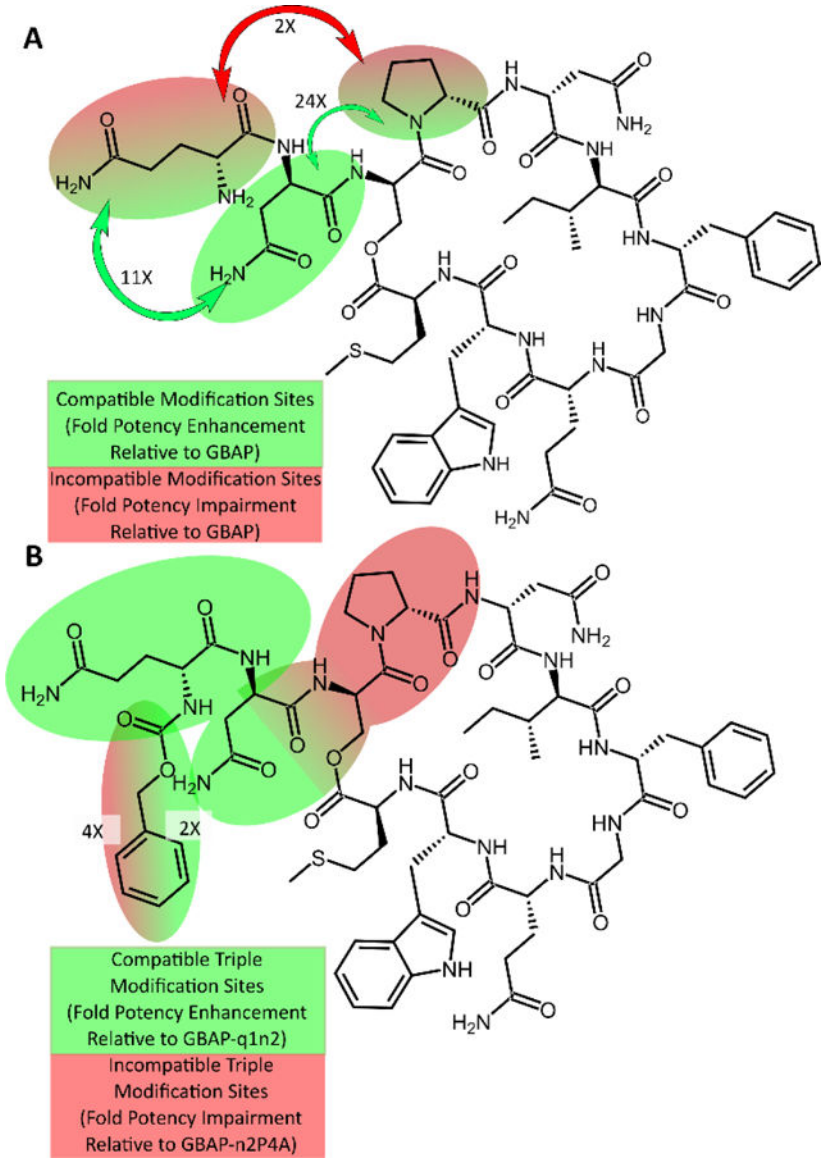

Figure 5.

Results of rational design on potency where green indicates improvement in potency and red indicates loss of potency, with numbers indicating the fold change in potency for the associated modifications. A) Analogs incorporating two modifications where arrows indicate the pairs of modifications made. B) Analogs incorporating the Z-group as a third modification where same-colored residues indicate the effect of their combined incorporation into the structure relative to the structure without the Z-group.

Table 1.

EC_{50} Values for Conservative Hydrophobic Ring Region Substitutions, Tail, and Cyclization Analogs[a]

Peptide #	Peptide Name	Sequence	EC_{50}[b] [95% CI][c](nM)	Fold Change[d]
1	GBAP[e]	QN(SPNIFGQWM)	1.15 [0.825 – 1.59]	NA
2	GBAP-G8A[e]	QN(SPNIF**A**QWM)	> 10,000	**(> 10,000)**
3	GBAP-G8a[f]	QN(SPNIF**a**QWM)	20.8 [8.65 – 50.1]	**(18)**
4	GBAP-f7[e]	QN(SPNIfGQWM)	4.97 [3.12−7.77]	**(4.3)**
5	GBAP-F7W	QN(SPNI**W**GQWM)	0.905 [0.625 – 1.31]	**1.3**
6	GBAP-F7w	WN(SPNI**w**GQWM)	1.82 [0.710 – 4.64]	**(1.6)**
7	GBAP-F7WW10F	QN(SPNI**W**GQ**F**M)	27.4 [17.7 – 42.4]	**(24)**
8	GBAP-W10F	QN(SPNIFGQ**F**M)	4.86 [3.43 – 6.89]	**(4.2)**
9	GBAP-F7AW10A[g]	QN(SPNI**A**GQ**A**M)	> 10,000	**(> 10,000)**
10	Ac-GBAP-Des(Q1N2)[e]	(SPNIFGQWM)	1.01 [0.496 – 2.06]	**1.1**
11	GBAP-Des(Q1N2) lactam[e,h]	(SPNIFGQWM)	> 10,000	**(> 10,000)**
12	GBAP-s3[e]	QN(**s**PNIFGQWM)	45.1 [17.0 – 120]	**(39)**
13	Ac-GBAP-Des(Q1N2)s3	**Ac-(s**PNIFGQWM)	7.58 [2.95 – 19.5]	**(6.6)**
14	GBAP-Des(Q1N2)s3 lactam[h]	(**s**PNIFGQWM)	764 [446 – 1311]	**(664)**
15	GBAP-Q1[pyroglutamate]	**[PyGlu]**-N(SPNIFGQWM)	1.14 [0.818 – 1.59]	**1.0**
16	GBAP-q1[pyroglutamate]	**[D-PyGlu]-**N(SPNIFGQWM)	3.11 [2.05 – 4.72]	**(2.7)**
17	Z-GBAP	**Z-**QN(SPNIFGQWM)	0.178 [0.080 – 0.397]	**6.5**
18	Z-GBAP-Des(Q1N2)	**Z-**(SPNIFGQWM)	0.661 [0.305 – 1.43]	**1.7**

[a] See experimental section for details of reporter strain and methods. All assays performed in triplicate.

[b] EC_{50} values determined by testing peptides over a range of concentrations.

[c] 95% confidence interval.

[d] Relative to GBAP, blue indicates improvement in potency, red plus parentheses indicates loss in potency.

[e] Previously published analog shown for comparison, see reference 3 for details.

[f] Lower case letters indicate residues replaced with the D enantiomer.

[g] Previously published analog whose activity was confirmed in the course of this study, see reference 26 for details.

[h] Lactam (head-to-tail) cyclization.

Table 2.

EC_{50} Values for Rationally Designed GBAP-Based Super Agonists[a]

Peptide #	Peptide Name	Sequence	EC_{50}[b] [95% CI][c] (nM)	Fold Change[d]
19	GBAP-q1n2[e]	**qn**(SPNIFGQWM)	0.103 [0.043 – 0.249]	**11**
20	GBAP-q1P4A	**q**N(S**A**NIFGQWM)	1.87 [1.24 – 2.81]	**(1.6)**
21	GBAP-n2P4A	Q**n**(S**A**NIFGQWM)	0.0460 [0.0300 – 0.0691]	**25**
22	GBAP-q1n2P4A	**qn**(S**A**NIFGQWM)	17.0 [10.3 – 28.0]	**(14.8)**
23	Ac-GBAP-q1	**Ac-q**N(SPNIFGQWM)	0.314 [0.112 – 0.880]	**3.7**
24	Ac-GBAP-n2	**Ac**-Q**n**(SPNIFGQWM)	1.47 [0.737 – 2.93]	**(1.3)**
25	Ac-GBAP-P4A	**Ac**-QN(S**A**NIFGQWM)	1.35 [0.704 – 2.59]	**(1.2)**
26	Ac-GBAP-q1n2	**Ac-qn**(SPNIFGQWM)	0.504 [0.220 – 1.16]	**2.3**
27	Ac-GBAP-q1P4A	**Ac-q**N(S**A**NIFGQWM)	3.51 [1.16 – 10.6]	**(3.1)**
28	Ac-GBAP-n2P4A	**Ac**-Q**n**(S**A**NIFGQWM)	0.590 [0.257 – 1.35]	**1.9**
29	Ac-GBAP-q1n2P4A	**Ac-qn**(S**A**NIFGQWM)	42.1 [29.9 – 59.3]	**(36.6)**
30	Z-GBAP-q1n2	**Z-qn**(SPNIFGQWM)	0.0623 [0.0269 – 0.144]	**19**
31	Z-GBAP-n2P4A	**Z**-Q**n**(S**A**NIFGQWM)	0.169 [0.096 – 0.295]	**6.8**

[a] See experimental section for details of reporter strain and methods. All assays performed in triplicate.

[b] EC_{50} values determined by testing peptides over a range of concentrations.

[c] 95% confidence interval.

[d] Relative to GBAP, blue indicates improvement in potency, red plus parentheses indicates loss in potency.

[e] Lower case letters indicate residues replaced with the D enantiomer.

Table 3.

IC_{50} Values for Tail-Modified Antagonists and Rationally Designed GBAP-Based Enhanced Antagonists[a]

Peptide #	Peptide Name	Sequence	IC_{50}[b] [95% CI][c] (nM)
32	Z-GBAP-N5[YBzl]Q9AM11A[d]	**Z**-QN(SP-**YBzl**-IFG**A**W**A**)	> 10,000[e], >10,000[f]
33	Ac-GBAP-N5[YBzl]Q9AM11A	**Ac**-QN(SP-**YBzl**-IFG**A**W**A**)	> 10,000[e]
34	Ac-GBAP-Des(Q1N2)N5[YBzl]Q9AM11A	Ac-(SP-YBzl-IFGAWA)	> 10,000[e]
35	GBAP-N5[YBzl]M11A	QN(SP-**YBzl**-IFGQW**A**)	139 [61.8 – 313][e]
36	Z-GBAP-N5[YBzl]M11A	**Z**-QN(SP-**YBzl**-IFGQW**A**)	227 [172 – 299][e], 38.7 [26.8 – 55.9][f]
37	GBAP-Q1[pyroglutamate]N5[YBzl]M11A	[PyGlu]-N(SP-YBzl-IFGQWA)	295 [232 – 375][e]
38	Ac-GBAP-N5[YBzl]M11A	**Ac**-QN(SP-**YBzl**-IFGQW**A**)	444 [25 – 918][e]
39	Ac-GBAP-Des(Q1N2)N5[YBzl]M11A	**Ac**-(SP-**YBzl**-IFGQW**A**)	872 [520 – 1463][e]
40	Z-GBAP-q1n2N5[YBzl]M11A[g]	**Z-qn**(SP-**YBzl**-IFGQW**A**)	388 [183 – 826][e]
41	Z-GBAP-n2P4AN5[YBzl]M11A	**Z**-Q**n**(S**A**-**YBzl**-IFGQW**A**)	> 10,000[e]
42	GBAP-q1n2N5[YBzl]M11A	**qn**(SP-**YBzl**-IFGQW**A**)	967 [729 – 1281][e]
43	GBAP-n2P4AN5[YBzl]M11A	Q**n**(S**A**-**YBzl**-IFGQW**A**)	> 10,000[e]
44	GBAP-N5[YBzl]	QN(SP-**YBzl**-IFGQWM)	438 [225 – 853][e]
45	Z-GBAP-N5[YBzl]	**Z**-QN(SP-**YBzl**-IFGQWM)	> 1,000[e]
46	GBAP-q1n2N5[YBzl]	**qn**(SP-**YBzl**-IFGQWM)	> 10,000[e]
47	GBAP-n2P4AN5[YBzl]	Q**n**(S**A**-**YBzl**-IFGQWM)	> 1,000[e]

[a] See experimental section for details of reporter strain and methods. All assays performed in triplicate.

[b] IC_{50} values determined by testing peptides over a range of concentrations.

[c] 95% confidence interval.

[d] Previously published analog showed different activity than observed in our hands, see reference 27.

[e] 50 nM GBAP as competitor.

[f] 5 nM GBAP as competitor.

[g] Lower case letters indicate residues replaced with the D enantiomer.